Separation Science and Technology
Publication details, including instructions for authors and subscription information:
http://www.informaworld.com/smpp/title~content=t713708471

Separation of Nitrocellulose-Manufacturing Wastewater by Bench-Scale Flat-Sheet Crossflow Microfiltration Units

X. Shen[a]; J. K. Park[a]; B. J. Kim[b]
[a] DEPARTMENT OF CIVIL AND ENVIRONMENTAL ENGINEERING, UNIVERSITY OF WISCONSIN-MADISON, MADISON, WISCONSIN [b] U.S. ARMY CORPS OF ENGINEERS, CHAMPAIGN, ILLINOIS

To cite this Article Shen, X. , Park, J. K. and Kim, B. J.(1994) 'Separation of Nitrocellulose-Manufacturing Wastewater by Bench-Scale Flat-Sheet Crossflow Microfiltration Units', Separation Science and Technology, 29: 3, 333 — 356
To link to this Article: DOI: 10.1080/01496399408002487
URL: http://dx.doi.org/10.1080/01496399408002487

SEPARATION SCIENCE AND TECHNOLOGY, **29**(3), pp. 333–356, 1994

Separation of Nitrocellulose-Manufacturing Wastewater by Bench-Scale Flat-Sheet Crossflow Microfiltration Units

X. SHEN and J. K. PARK*
DEPARTMENT OF CIVIL AND ENVIRONMENTAL ENGINEERING
UNIVERSITY OF WISCONSIN-MADISON
MADISON, WISCONSIN 53706

B. J. KIM
U.S. ARMY CORPS OF ENGINEERS
CHAMPAIGN, ILLINOIS 61820

ABSTRACT

This paper reports laboratory-scale experiments for the separation of nitrocellulose fines from nitrocellulose manufacturing wastewater with crossflow microfiltration units. Results are reported in terms of the factors affecting permeate flux, membrane fouling, the effects of pulsating cleaning and chemical cleaning, and the optimum condition for operation. The separation process under steady operation is described mathematically with the aim of elucidating the transport mechanism and the effects of operating parameters on permeate flux.

INTRODUCTION

The nitrocellulose (NC)-manufacturing wastewater generated from the Radford Army Ammunition Plant (RAAP) contains a suspended solids concentration of 80 to 900 ppm, and approximately 2 tons of solids escape daily as the effluent from one of the lines. The source of the process wastewater include: acid boiling, poaching, blending, and wringing operations. The wastewater is neutral to slightly alkaline and contains a mixture of short fibers and colloidal fines. Currently 24 sliding bowl centrifuges

* To whom correspondence should be addressed.

are installed to separate NC fines in the discharge stream. However, they are unable to obtain the maximum acceptable level of 25 ppm proposed by the Ammunition Procurement and Supply Agency (APSA). Therefore, some practical and economical means must be sought to separate NC fines to achieve the proposed APSA standard.

Although toxicity data shows that nitrocellulose has low toxicity in mammalian systems (1), nitrocellulose may produce significant abiotic environmental effects (2). Additionally, because of its extreme flammability, NC-manufacturing sludge is listed as hazardous waste. The present National Pollutant Discharge Elimination System (NPDES) sets limits for the NC at RAAP at an average of 40 ppm for a 24-hour composite sample. However, the State of Virginia may demand more stringent limitations in the future. There have been only limited research and development efforts for NC waste treatment and disposal despite the fact that NC production technology development has a long history. It is desirable to develop new technologies with higher reliabilities and lower operating costs to meet more stringent discharge permits in the future.

A study (3) recommended that crossflow microfiltration is one of the most suitable techniques for NC waste separation. The alternatives compared were: solid bowl centrifugation, conventional pressure filtration, slide bowl centrifugation, and crossflow microfiltration. Only limited tests were conducted by microfilter manufactures. Therefore, it is necessary to conduct further study for assessing the feasibility of using crossflow microfiltration for NC fine removal.

Crossflow microfiltration is a relatively new membrane filtration technology. Accordingly, very little work has been done on the performance of crossflow microfiltration during solid–liquid separation, not to mention NC fine filtration. Principally, crossflow filtration affords the possibility of a steady or a quasi-steady operation with nearly constant flux when the driving pressure difference is held constant. Due to membrane fouling, however, crossflow alone does not suffice to maintain sufficient flow of a permeate over an extended period of time. Physical blocking of the pores of a membrane, adsorption of materials on the membrane surface, and polarization, i.e., gel layer formation, have been identified as the main problems causing resistance to solvent transport. In addition, separation characteristics and sensitivity of membranes to fouling are very dependent on the nature of the fluid being processed and the morphology of the membrane, as well as to process configuration. As a result, a laboratory investigation was conducted to explore the feasibility of crossflow microfiltration of NC-manufacturing wastewater and to yield the necessary data for the assessment of the applicability.

The main objectives of this study were: 1) to assess the removal efficiency of NC fines for an extended period of time; 2) to investigate the performance of various membranes in terms of flux drop and transmembrane pressure difference; 3) to determine factors affecting permeate flux; 4) to find methods of fighting fouling and extending membrane life; and 5) to understand the physical phenomena governing flux and explain experimental observations, which may lead to the development of a theoretical model.

EXPERIMENTAL

Nitrocellulose

NC is produced by the reaction of cellulose with mixtures of nitric acid (21–23%), sulfuric acid (59–67%), and water (10–20%) in a reversible process to form the nitrate ester of cellulose, designated NC. The nitration of cellulose can be expressed as follows (4):

$$C_6H_{10}O_5 + xHNO_3 \leftrightarrow C_6H_{10-x}O_{5-x}(ONO_2)_x + xH_2O \quad (1)$$

The cellulose formula in this equation is simplified by assuming a polymerization degree of $n = 1$. The degree of nitration is determined by batch contact time, mixed acid ratios, and the cellulosic backbone with a maximum theoretical yield of 14.15% N by weight. In practice, NC polymers containing between 12.6 and 13.4% N are designated as "gun cotton" or "smokeless powder" and are used as propellants in the pyrotechnic industry. Due to its cellulose backbone, NC is not a simple chemical compound but rather it is a class of nitrated cellulose polymers defined by the physical-chemical properties indicated below (5).

Molecular weight: variable, $273.3n$, where n is the degree of polymerization
Chemical formula: $(C_6H_{10-x}O_{5-x}(ONO_2)_x)_n$ for 12.6% N, $x = 2.45$
Color: white
Density: ~1.66 g/cm^3
Solubility: acetone, ether:alcohol (2:1), nitro compounds, organic nitrates, fatty acid esters, insoluble in water
Flash point: 4°C (closed cup)
Glass transition temperature (T_g): 53 to 66°C (6)
Heat of combustion: 2409 kcal/kg

If NC with a high degree of substitution is immersed in an acid mixture that would produce a lower degree of substitution at equilibrium, then NC will be denitrated to the equilibrium level (7). The molecular weight

of NC in the NC-manufacturing waste ranged from 58,000 to 480,000 g/mol with a nitrogen content of 11.9 to 13.1% (8, 9).

The zeta potential of a composite NC-manufacturing wastewater sample ranged from −16.5 to −28.8 mV, and the isoelectric point was approximately pH 1.9 (10). The particle sizes between 3 and 20 μm accounted for 94% by weight of the NC-manufacturing wastewater. The average NC particle size based on the volume measurement by a particle size analyzer was 9.3 μm. However, NC particle sizes ranging from 0.5 to 1.5 μm accounted for almost 70% of NC fines counted by the particle size analyzer.

Description of Experimental System

The properties of the membranes used in the experiments are summarized in Table 1. Two types of flat-sheet membrane module were used. The specifications of the modules and feed pumps are provided in Table 2. The experiments were operated either in a closed loop mode or in a modified batch.

In a closed loop mode, the flows of both the permeate and concentrated fluxes were recycled to the supply vessel; thus, there was no change in suspended solids concentration. In a modified batch mode, the feed was supplied from a constant volume tank whose liquid level was kept unchanged by incoming fresh wastewater and the concentrate leaving the membrane and recirculating into the system. This resulted in an increase in suspended solids concentration in the supply vessel.

To perform pulsating cleaning, three solenoid values were used: one (normally open) in the concentrate line, another (normally open) in the permeate line, and the third (normally closed) in the by-pass line. An automatic timer was provided to close and open these valves at required

TABLE 1
Properties of Membranes Used

Properties	Membranes					
Type	GVLP	HVLP	PVLP	GLSR	GLSR	MMP-601
Manufacturer	Millipore	Millipore	Millipore	Amicon	Amicon	Koch
Pore size	0.2 μm	0.45 μm	0.65 μm	0.22 μm	0.45 μm	1.0 μm
Material	PVDF[a]	PVDF[a]	PVDF[a]	PS[b]	PS[b]	PS[b]
Configuration	Flat sheet	Flat sheet	Flat sheet	Flat sheet	Flat sheet	Flat sheet
Comments	—	—	—	—	—	Research membrane

[a] PVDF: polyvinylidene difluoride.
[b] PS: polysulfone.

TABLE 2
Specifications of Filtration Apparatus

Specifications	Crossflow plate-and-frame apparatus	
Type	Minitan-S	Model TM-100
Manufacturer	Millipore	New Brunswick Scientific Co. Inc.
Materials	Stainless steel frame acrylic manifolds	Stainless steel frame polypropylene manifolds
Filter area	30 cm^2	64.5 cm^2
Hold-up volume	10 mL	2 mL
Dimensions	6″ (L) × $4\frac{1}{2}$″ (W) × $4\frac{3}{4}$″ (H)	$7\frac{3}{4}$″ (L) × $4\frac{1}{3}$″ (W) × $9\frac{1}{2}$″ (H)
Pump	Cole-Parmer Pumphead: Masterflex, Model 7016-20	Gear pump drive Pumphead: Micropump

time intervals. Figure 1 shows a schematic arrangement for pulsation of flux. During filtration (on), V_1 and V_2 were opened while V_3 was closed. During pulsating cleaning (off), V_1 and V_2 were closed while V_3 was opened. The details of solenoid valve operation are shown in Fig. 2. Operational parameters used in this experimental study are summarized in Table 3.

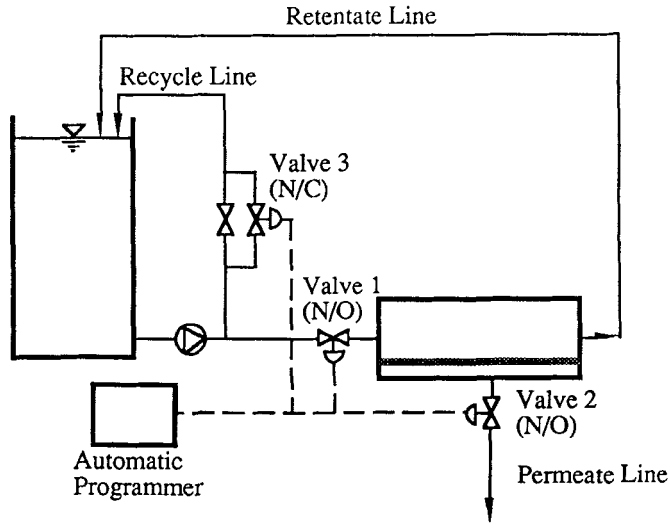

FIG. 1 Arrangement for pulsating cleaning. N/O = normally open valve. N/C = normally closed valve.

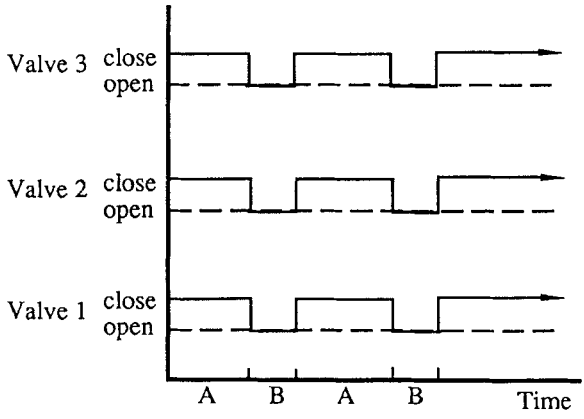

FIG. 2 Mode of solenoid valve operation.

Analytical

The experiments were performed with NC-manufacturing wastewater coming from the overflow of the poacher pit at RAAP. The feed and permeate samples were analyzed for turbidity, total suspended solids (TSS), and pH. TSS determination procedures used adhered to the Temporary Procedure #L-395—Determination of TSS in NC Waste established by Hercules Inc. (11) based on a weighing method. Turbidity was measured with the use of DRT-100B Turbidimeter (H.F. Scientific Inc.). TSS was found to have the following relationship in the turbidity range

TABLE 3
Experimental Conditions

Membrane pore diameter	0.2, 0.45, 0.65, 1.0 μm
NC wastewater analysis:	
Turbidity	380–450 NTU
TSS	300–355 mg/L
pH	7.5
Permeate flux	80–700 L/h·m^2
Tangential velocity	0.37–1.19 m/s
Transmembrane pressure drop	0.5–10 psi
Pulsating cleaning:	
Pulsating cycle	2/1, 3/1 (on/off)
Pulsation breakdown	1/3, 1, 2 min
Chemical cleaning	Tergazime 0.5% or Tergazime + NaOH (pH ~10)
Ambient temperature	~22°C

TABLE 4
Weight Distribution of NC Fines by Size

NC fine size (μm)	Weight (mg)	Weight (%)
210<	1.0	0.64
210–70	0.9	0.58
70–41	1.7	1.10
41–30	0.5	0.32
30–20	3.7	2.37
20–10	105.6	67.79
10–3	40.7	26.12
3–0.7	1.3	0.81
0.7–0.45	0.4	0.27

between 10 to 400 NTU (Nephelometric turbidity unit):

$$\text{TSS (mg/L)} = 0.778 \text{ turbidity (NTU)} + 3.475 \quad (r^2 = 0.9995) \quad (2)$$

Another important characteristic of NC fines which is vital in selecting microfiltration membranes is their average particle size distribution. A particle size analysis was performed by passing a sample through sieves and filters of different pore diameters and determining the weight of the collected material. The weight distribution as a function of the particle size is provided in Table 4. A particle size analyzer (PSA) (Brinkmann Instruments Inc.) was also used to estimate the average size and distribution of relative sizes of the particles found in the sample based on the volume distribution. The average size of the NC particle by volume was approximately 8 μm, in good agreement with the result obtained from weight distribution. Additionally, the NC particle size < 0.45 μm was measured by a microscope. It was found from the microscopic observation that particles less than 0.5 μm were negligible.

RESULTS AND DISCUSSION

Factors Affecting Permeate Flux

The influence of the crossflow velocity of the fluid, u_b, in the flat-sheet membrane on the permeate flux, J, was investigated at a transmembrane pressure difference of 2 psi and a constant feedwater NC fine content (400 NTU) by the use of a closed loop operation mode. The changes in the permeate flux as a function of the operation time for three different crossflow velocities of 0.37, 0.82, and 1.19 m/s are shown in Fig. 3. The Megaflow Membrane Filtration Apparatus (Model TM100) was used with the membrane of GLSR-Amicon, 0.45 μm.

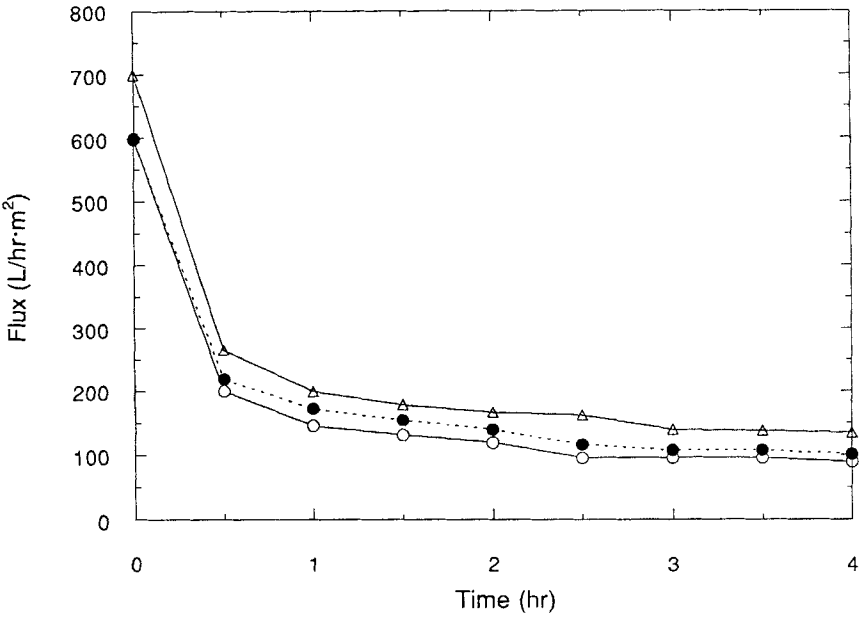

FIG. 3 Effect of crossflow velocity on permeate flux (conditions: turbidity of feedwater = 400 NTU, ΔP = 2 psi, operation mode = closed loop). Crossflow velocity (in m/s): (○) 0.37, (●) 0.82, (△) 1.19.

The increase in the crossflow velocity generally resulted in a flux increase and retardation of flux decay by reducing the cake mass deposited on the membrane surface. The deposition layer thickness in the crossflow microfiltration was controlled by the crossflow velocity, as expected. In general, the flux is proportional to the average tangential flow velocity. The dependence of the flux on the crossflow velocity has been known to be dominated by the flow regime in the channel (12, 13). The permeate flux was found to be a function of $u_b^{1/3}$. In the flat-sheet membrane module used in this situation, a laminar-flow regime appeared to be formed since the Reynolds number was smaller than 2320.

One of the problems in using high tangential velocity to increase the flux is the concomitant increase in the transmembrane pressure drop, ΔP, which would adversely affect the membrane performance. In addition, the effect of crossflow is diminished at high u_b values. Baker (12) found that the specific resistance increased significantly as u_b reached high values. As a result, the crossflow velocity of approximately 1.07 m/s was thought to be adequate for this application when a flat-sheet module was used.

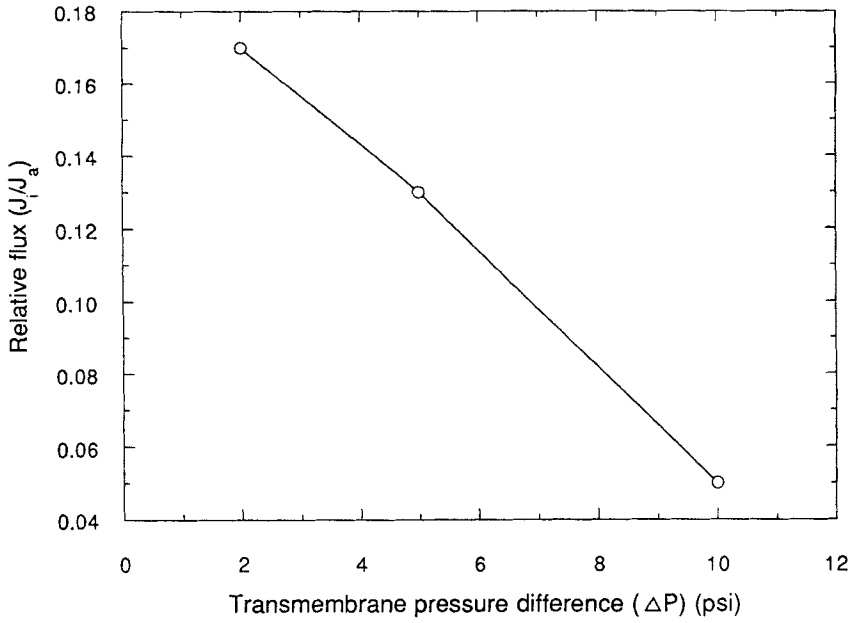

FIG. 4 Effect of transmembrane pressure drop on permeate flux (conditions: crossflow velocity = 0.82 m/s, turbidity of feedwater = 400 NTU, operation mode = closed loop).

The influence of transmembrane pressure drop on the permeate flux was investigated at a constant crossflow velocity (0.82 m/s) and a constant NC fine content of the feed water (400 NTU).

The relative flux, defined as the ratio between the actual permeate flux after 4-hour operation time, J_a and the initial permeate flux, J_i, was plotted as a function of the transmembrane pressure difference in Fig. 4. It can be said that the relative flux decreased with the increased transmembrane pressure difference due to the effect of membrane fouling. Initially, the increase in ΔP boosted the permeate flux but accelerated the flux drop in the later phase. This flux drop can be explained by the membrane fouling resistance developed during the process filtration.

The increased transmembrane pressure difference provides an additional driving force for higher permeate flux. Thus, particles are initially transported at a great rate to the membrane, resulting in an increased internal membrane fouling resistance, conforming to the standard blocking model written as (14):

$$J = \Delta P/\mu(R_m + R_{if}) \tag{3}$$

where J = permeate flux, m/s
ΔP = transmembrane pressure drop (driving force), N/m^2
μ = viscosity of feed solution, kg/m·s
R_m = membrane resistance, m^{-1}
R_{if} = internal membrane fouling resistance, m^{-1}

Later, when the membrane pore is sufficiently plugged with fine particles, the filtration process follows the cake filtration model (14), leading to the eventual formation of cake (particle deposit layer) on the membrane surface. At higher ΔP, compaction of the cake could result and the cake layer thickness increases, leading to increased external membrane fouling resistance, R_{ef} (14). The cake filtration model is thus given by

$$J = \Delta P/\mu(R_m + R_{if} + R_{ef}) \quad (4)$$

Hence it is suggested that the crossflow microfiltration of NC-manufacturing fines wastewater should be operated at the lowest possible transmembrane pressure difference.

Factors Affecting Membrane Fouling

Membrane fouling is the term used to describe the inorganic and/or organic deposit on surface and physical blocking of the pores of a membrane. It causes either a rise in transmembrane pressure drop or a decay in the permeate. Accordingly, the rise in ΔP or reduction in the permeate flux indicates the progression of membrane fouling.

A series of experiments was conducted to evaluate the effect of the permeate flux on membrane fouling under the same constant crossflow velocity using a modified batch operation mode. The Minitan-S flat cell unit (Millipore Co.) was used with a HVLP membrane.

The transmembrane pressure drop as a function of time of operation for three various permeate fluxes is shown in Fig. 5. From the experiment it was apparent that maintaining a higher permeate flux resulted in an increase of a sharper transmembrane pressure drop during the first hour, indicating the accelerated membrane fouling. A higher permeate flux yielded the transport of NC fines at a greater rate to the membrane. It was found that under the higher permeate flux condition, the thicker retained layer composed of densely packed NC fines was formed on the membrane surface. There was also an indication that pore blockage had occurred prior to the formation of the thicker retained layer. Microfiltration membrane pores were susceptible to blockage by NC fines due to the wide range of NC fine particle size distribution and the rod-shaped, soft and flexible NC fines. To avoid premature membrane fouling, it is

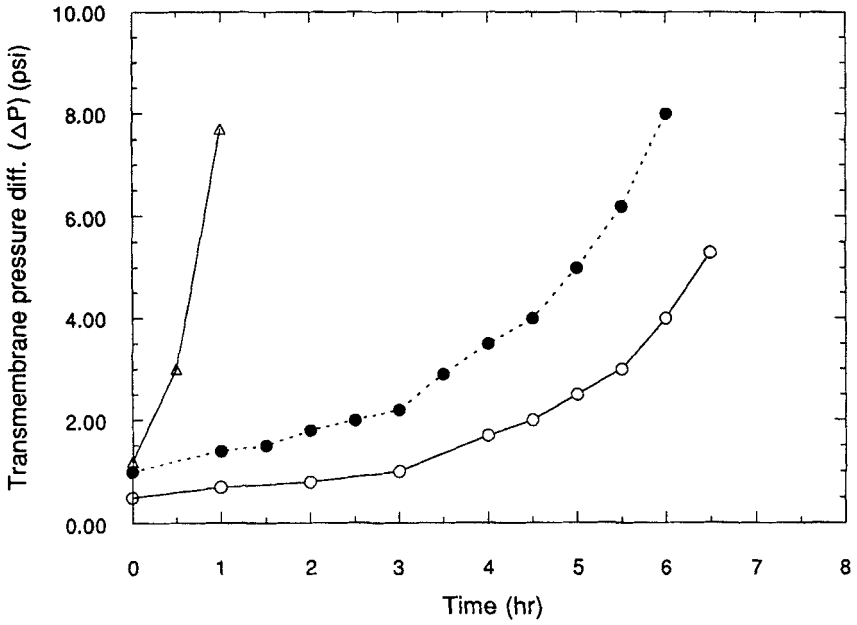

FIG. 5 Effect of permeate flux on transmembrane pressure drop (conditions: crossflow velocity = 0.82 m/s, operation mode = modified batch). Permeate flux (in L/h·m^2): (△) 678, (●) 240, (○) 180.

recommended to operate the crossflow microfiltration in a modest permeate flux (100–150 L/h·m^2).

The effect of membrane pore diameter on filtrate turbidity was studied at a constant NC fine concentration in the feedwater over a 4-hour running time using a closed loop operation mode. The results are summarized in Table 5. It can be seen that the difference in the filtrate turbidity among the various pore size membranes was marginal, especially after 0.5-hour of operation.

Another set of experiments was conducted with three different pore diameters—0.2, 0.45, and 0.65 μm—under a modified batch operation. The permeate flux was kept constant by increasing the transmembrane pressure during the operation time to observe the sensitivity of membrane fouling to the variation of pore sizes. The results are shown in Fig. 6. The turbidity of the filtrate was almost zero. Even in the initial period of time, it was far below the discharge limit for NC-manufacturing effluent of 40 mg/L. All the microfiltration membranes exhibited an initial period of filtration in which more NC fines appeared in the filtrate. After this period

TABLE 5
Variation of Filtrate Turbidity over Time Using Different Pore Size Membranes

Time (h)	Turbidity (NTU)			
	1.0 μm	0.65 μm	0.45 μm	0.2 μm
0.0	2.30	2.10	2.10	0.70
0.5	0.40	0.40	0.35	0.17
1.0	0.18	0.21	0.20	0.12
1.5	0.20	0.19	0.17	0.12
2.0	0.16	0.17	0.16	0.12
2.5	—	0.18	0.16	0.11
3.0	0.16	0.17	0.16	0.10
3.5	—	0.17	0.15	0.11
4.0	0.17	0.16	0.15	0.10

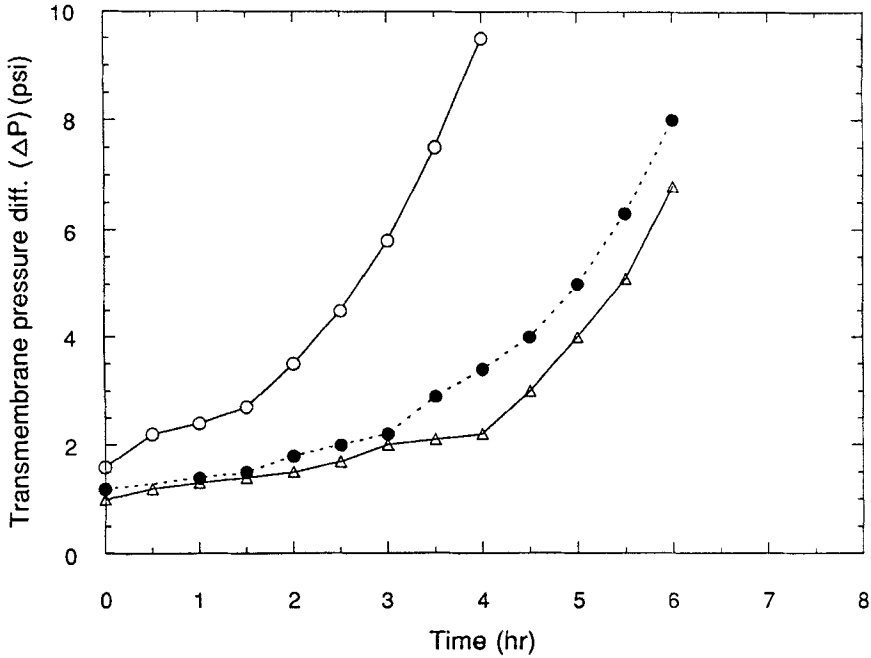

FIG. 6 Effect of membrane pore size on transmembrane pressure drop vs time relationship (conditions: permeate flux = 240 L/h·m^2, crossflow velocity = 0.82 m/s, operation mode = modified batch). Pore diameter (in μm): (○) 0.2, (●) 0.45, (△) 0.65.

the amount of NC fines in the membrane decreased and the permeate flux decayed. Furthermore, from the experiment it was apparent that the membrane of larger pore diameter was less sensitive to the increased turbidity, as shown in Fig. 6.

It is desirable to use as large a pore diameter as possible to maximize the microfiltration permeate flux; thus, a membrane of 0.6 μm pore diameter is recommended for the flat-sheet membrane microfilters used in this application. However, it should be noted that the conclusion is to some extent restricted by the current limited commercial availability of larger pore diameter membranes.

Membranes with two different pore diameters—0.2 and 0.65 μm—were tested to compare the rate of increase in ΔP for a constant feedwater NC fine concentration with that for a continuously increased feedwater NC fine concentration. A constant permeate flux was held with unchanged crossflow velocity to observe the rise in ΔP, i.e., progression of membrane fouling. The results are shown in Fig. 7. It can be seen that ΔP rose sharply while the feedwater was concentrated. Besides, smaller pore membrane appeared to be more sensitive to the increased NC fine concentration. The membrane with 0.2 μm pore size showed a much higher rate of ΔP increase (7 psi in 4 hours) with the final concentration factor of 6×. On the other hand, ΔP increase for the 0.65-μm pore diameter membrane was 6 psi in 6 hours with a final concentration factor of 8.5×.

The increased NC fine concentration of the feedwater created a higher membrane fouling rate. The increased turbidity, and thus the increased viscosity of the feed solution, in general would result in the deterioration of the permeate flux. The higher membrane fouling rate due to the increased turbidity of the feedwater shown in this experiment was most likely related to this flux deterioration.

Membrane Cleaning

Pulsating and chemical cleanings were attempted to combat membrane fouling. The pulsating cleaning technique was designed to minimize membrane fouling developed during the microfiltration of the NC-manufacturing wastewater. Shock waves were created through the membrane by closing and opening the valves at required time intervals, which were controlled by an automatic timer. The operation cycle used during the experiment was defined as time on/time off (see Figs. 1 and 2). The experiment was conducted with different cycles and different break durations (off). The results are shown in Fig. 8.

The permeate flux was improved when using pulsating cleaning compared with no pulsating cleaning based on the actual working hours under

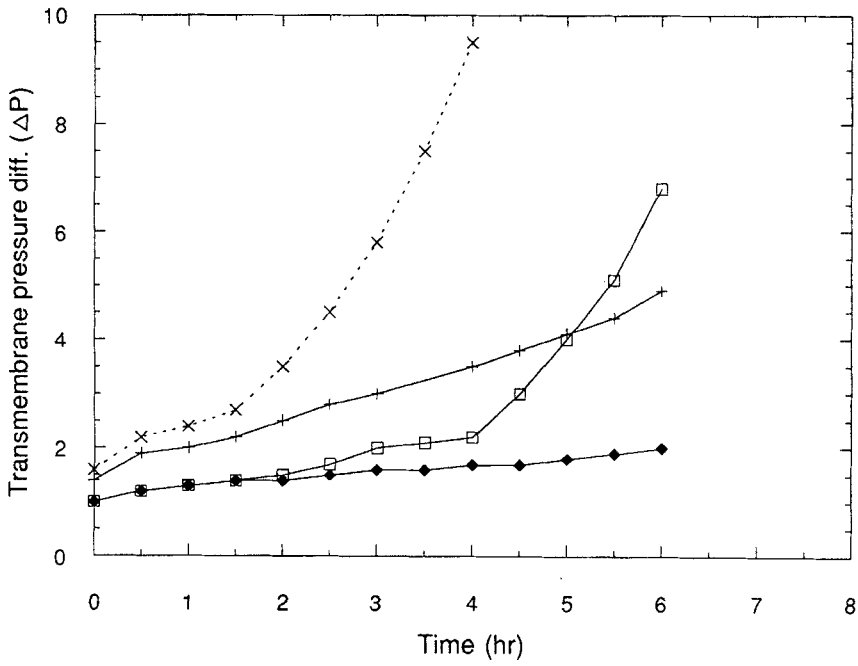

FIG. 7 Effect of feedwater turbidity on transmembrane pressure drop (conditions: permeate flux = 240 L/h·m^2, crossflow velocity = 0.82 m/s). ΔP as a function of time plotted with different conditions: (×) pore diameter = 0.2 μm, initial turbidity = 400 NTU, final concentration factor = 6×, operation mode = modified batch; (+) pore diameter = 0.2 μm, turbidity = 400 NTU, operation mode = closed loop; (□) pore diameter = 0.65 μm, initial turbidity = 400 NTU, final concentration factor = 8.5×, operation mode = modified batch; (◆) pore diameter = 0.65 μm, turbidity = 400 NTU, operation mode = closed loop.

similar operation conditions. The flux increased by 50% during a 7-hour operation when a running cycle of the on/off ratio of 2/1 with an off-time of 2 minutes was applied. The permeate flux behaviors as a result of pulsation, as shown in Fig. 8, suggest that a longer break duration would result in better improvement. In fact, pulsating cleaning operation worked as self-cleaning, which is probably an important measure to achieve a long-term practical flux level for such microfiltration modules as flat-sheet membrane modules where backflush is baffled due to its nonself-supporting structure of membrane.

Chemical cleaning of fouled membrane was attempted by the removal of membrane foulants using specific chemical agents. Membranes were cleaned chemically when the transmembrane pressure drop was greater than 10 psi. Pure water fluxes measured before and after cleaning were

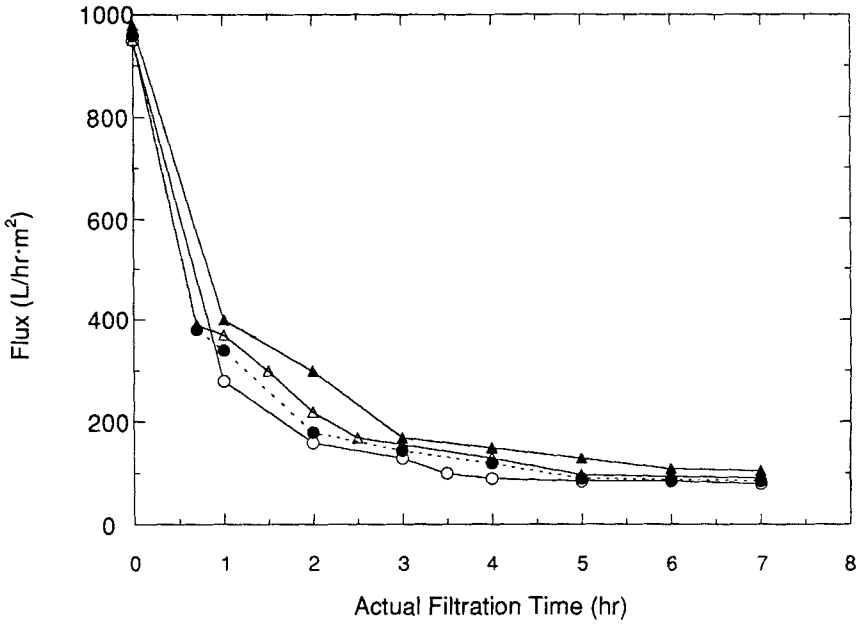

FIG. 8 Effect of pulsating cleaning on permeate flux (conditions: turbidity = 420 NTU, crossflow velocity = 90 m/s, ΔP = 2 psi, operation mode = closed loop). Flux as a function of time plotted with different conditions: (○) no pulsation; (●) pulsation cleaning, on/off = 1:0.3, off-time = 0.3 min; (△) pulsating cleaning, on/off = 2:1, off-time = 1 min; (▲) pulsating cleaning, on/off = 2:1, off-time = 2 min.

used as an indicator of the degree of cleaning. Different kinds of cleaning solutions were stirred in contact with the fouled membrane in a vessel at room temperature (22°C) for 5 hours to simulate a generally accepted clean-in-place procedure. Then the membrane was rinsed and flushed with pure water for approximately 15 minutes to wash out all the absorbed chemical agents.

It was found that a 0.5% Tergazyme solution by weight cleaned the fouled membrane best for the microfiltration membrane types—GVLP, HVLP, and DVLP—and a 0.5% by weight Tergazime solution plus NaOH to adjust pH to 10 for GLSR. The flux after clean-up achieved almost 90–100% of the initial pure water permeate flux.

Transport Mechanism

In view of the complex phenomena of permeate flux decline and membrane fouling shown in the present experimental studies, it is important

to explore theoretical models to understand and describe the transport mechanism governing the filtrate flux. To date, very few models proposed for filtrate flux have been adequate for explaining experimental observations or predicting device performance (15, 16).

In the earliest work in this area, crossflow microfiltration was regarded as a process where the carrier liquid is removed through a porous medium using pressure as the driving force and a particulate deposit on the separating medium. The cake filtration theory was applicable to a certain degree (17), but obviously limited since the shearing force caused by tangential flow was not considered. Other attempts included the application of the model used in the ultrafiltration process based on a concentration polarization concept where the drag force is balanced at steady-state by Brownian diffusivity of the particles. Application of this kind of the model, however, has shown significant discrepancies between the prediction of the model and experimental results.

The ultrafiltration model underestimates the filtrate flux of crossflow microfiltration, usually as much as two orders of magnitude lower than that of actual observations (16) because the value of the Brownian diffusion coefficient, which is inversely proportional to the particle radius, is quite small even for micrometer-sized particles. Various models were developed to modify the ultrafiltration model, such as the model based on the theory of shearing-induced hydrodynamic diffusion arising from particle–particle hydrodynamic interaction. Zedney and Colton proposed the following model to incorporate shear-enhanced diffusivity of a large floc (18):

$$J = 0.078 \left(\frac{a^4}{L}\right)^{1/3} \gamma_w \ln\left(\frac{C_w}{C_b}\right) \tag{5}$$

where J = length average flux, cm/s
a = particle radius, cm
γ_w = wall shear rate, s^{-1}
C_w = particle content at wall, dimensionless
C_b = particle content in bulk solution, dimensionless
L = channel length, cm

Zedney and Colton claimed that agreement with experiments was good for membrane plasmapheresis; however, the model did not include the effects of particle deformability and the hydraulic resistance of the particle layer at the membrane. Besides, it is impracticable to define particle radius in the case where a wide range of particle size distribution exists.

It was thought that the model for crossflow microfiltration used in the separation of particle suspensions could be a hybrid somewhere between basic filtration and ultrafiltration, which incorporates the concepts of diffusivity (backtransport) and the known equation of the filtration theory such as Eq. (4). For an approximation, the membrane resistance and internal resistance, which are relatively insignificant in comparison with the external resistance under a steady or a quasi-steady operation, can be neglected and thus Eq. (4) becomes

$$J = \Delta P/\mu R_{ef} \tag{6}$$

Since the resistance of the particle deposit is proportional to its thickness, δ, and the specific resistance of the layer, r, R_{ef} may be defined as

$$R_{ef} = r\delta \tag{7}$$

Hence,

$$J = \Delta P/\mu r\delta \tag{8}$$

In the steady-state condition, the retained material of the suspended particles transported toward the membrane (convection) is balanced by the material of the suspended particles transported back into the bulk stream because of shear-induced hydrodynamic diffusion. On the basis of mass balance, the transport rate by convection can be described as

$$m = J\frac{\rho}{\rho - C_s}C_s \tag{9}$$

where m = mean flow of the retained material, kg/m^2·s
ρ = density of particle deposit layer, kg/m^3
C_s = concentration of particle in bulk stream, kg/m^3

For the backtransport, it is assumed that this rate is proportional to the velocity gradient, du/dy, on the membrane and cake-layer thickness, δ:

$$m = \kappa\delta\frac{du}{dy}\rho \tag{10}$$

The mass balance for steady-state can be expressed as

$$J\frac{\rho}{\rho - C_s}C_s = \kappa\delta\frac{du}{dy}\rho \tag{11}$$

For the Newtonian fluid, du/dy is found to be a function of shear stress, τ, and fluid viscosity, μ:

$$\frac{du}{dy} \propto \frac{\tau}{\mu} \tag{12}$$

In the case of laminar flow, shear stress is not only proportional to the tangential velocity, u_b, but also depends on μ and the channel half-height, h:

$$\tau = 3\frac{\mu}{h}u_b \tag{13}$$

Equations (8) and (11) lead to the following equation for the permeate flux:

$$J = \sqrt{\frac{K\Delta P u_b(\rho - C_s)}{\mu r h C_s}} \tag{14}$$

where J = permeate flux, m/s
ΔP = transmembrane pressure drop, Pa
ρ = density of particle deposit layer, kg/m^3
u_b = tangential fluid velocity, m/s
C_s = concentration of particle in bulk stream, kg/m^3
μ = dynamic viscosity of fluid, Pa·s
r = specific deposit layer resistance, m^{-2}
h = half-height of flow channel, m
K = dimensionless constant

A similar model based on filtration theory has been proposed by Schulz and Ripperger (13). Equation (14) was derived for a flat-sheet microfilter operated in a lower Reynolds number (<2320).

In crossflow microfiltration, membrane fouling and concomitant flux decline strongly depend on the physical property of particles, membrane morphology, and the interaction between particles and membrane. It is difficult to define real pores and smooth geometric surface at the micrometric level. The situation is complicated by the wide range of particle size distribution and the peculiar characteristics of NC fine such as the shape and deformability. Nevertheless, fouling leads to an increase of the resistance to permeate by thickening and/or compression of the particle deposit layer, which are included in Eq. (14), as r, the specific resistance. It is clear from Eq. (14) that the transmembrane pressure drop and crossflow velocity at steady-state are reduced to a certain extent by the tendency of formation of a particle deposit layer of increased high specific resistance. Obviously, if the particle causing blockage and formation of a cake layer did not limit the permeate flux, the flux should increase with increased transmembrane pressure drop, contrary to the experimental results. In addition, specific resistance was dependent on the crossflow ve-

locity. The effect of crossflow was diminished at a high u_b value due to the significant increase of specific cake resistance arising from the exclusion of large particles from the cake (12, 19).

The permeate flux is related to the channel half-height, h, which would be decreased due to particle deposition and the build-up of cake thickness. The decrease causes an increase in shear stress since the same volume of suspension must flow through a more restricted channel, thus leading to an increase in diffusivity, which in turn will balance the rate of particle deposition on the layer. Variation in the particle concentration, C_s, and the viscosity of fluid, which is a strong function of C_s, will complicate the dynamic equilibrium. This effect is incorporated in Eq. (14). Davis and Birdsell showed that the cake layer thickness increased with particle concentration in the bulk stream (20). The adverse influence of increased C_s on membrane performance was also observed in the experiments mentioned above.

In summary, this model was found to be adequate as an explanation of

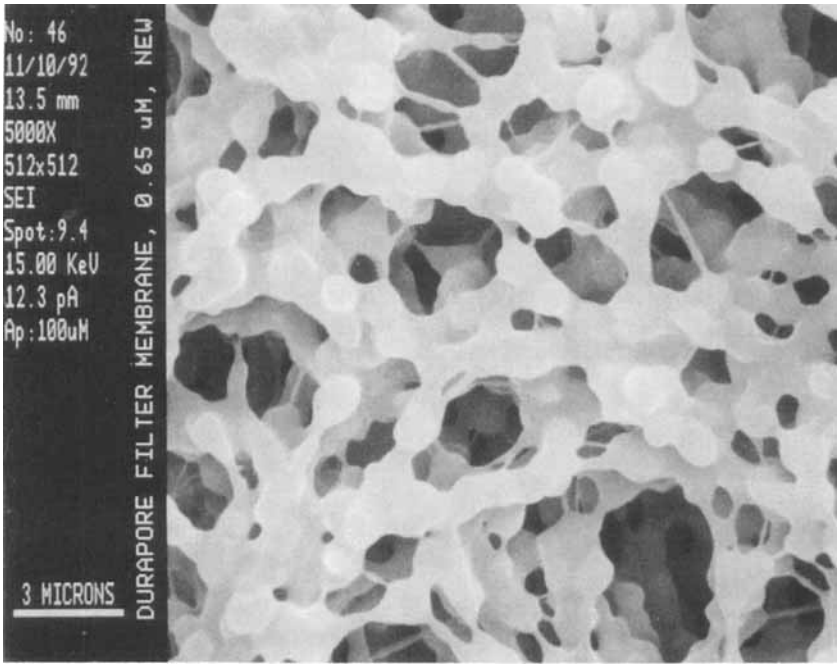

FIG. 9 SEM picture of the top layer of an M-F membrane of Type PVLP—Durapore (0.65 μm).

the foregoing experimental observation, although a detailed quantitative comparison of the model was not made with the experimental data. The model incorporating shear-induced hydraulic diffusion and cake filtration theory is expressed in terms of such macroscopic properties as tangential fluid velocity, transmembrane pressure drop, specific resistance, fluid viscosity, and permeate flux, all of which are evaluated from experimental measurements. The value of specific resistance must be known in order to predict permeate performance. A range of 1×10^{16} to 1×10^{17} m^{-2} of r in steady-state or quasi-steady-state operation was calculated in our experiment.

Electron Microscopy

Scanning electron microscopy was used to characterize fouled membranes as well as the structure of microfiltration membranes. Figures 9

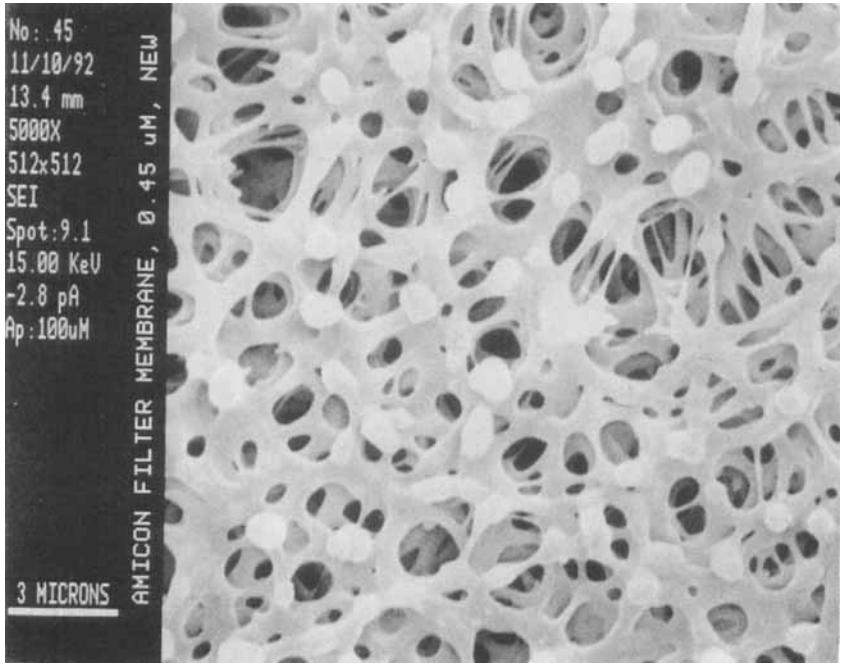

FIG. 10 SEM picture of the top layer of an M-F membrane of Type GLSR—Amicon (0.45 μm).

and 10 show top views of the MF-Millipore (0.65 μ) and MF-Amicon (0.45 μ). The membranes not only had high porosity but also had rough surfaces. A sponge-like and tortuous microporous structure can be seen.

Membrane fouling was examined after a long-term run when the transmembrane pressure difference had risen to over 10 psi. In Fig. 11 the top cake layer formed, which has a thickness of about 80 μm, on the membrane can be seen from a cross-sectional view. Figure 12 shows a top view of the surface of the fouled membrane with further magnification. It can be seen that the cake layer is composed of densely packed debris of NC fines.

Deposition of particles of different shapes and sizes on the top surface was examined. It can be seen from Fig. 13 that particles smaller than the size of pores are trapped in the pores, bridging the openings of the surface pores.

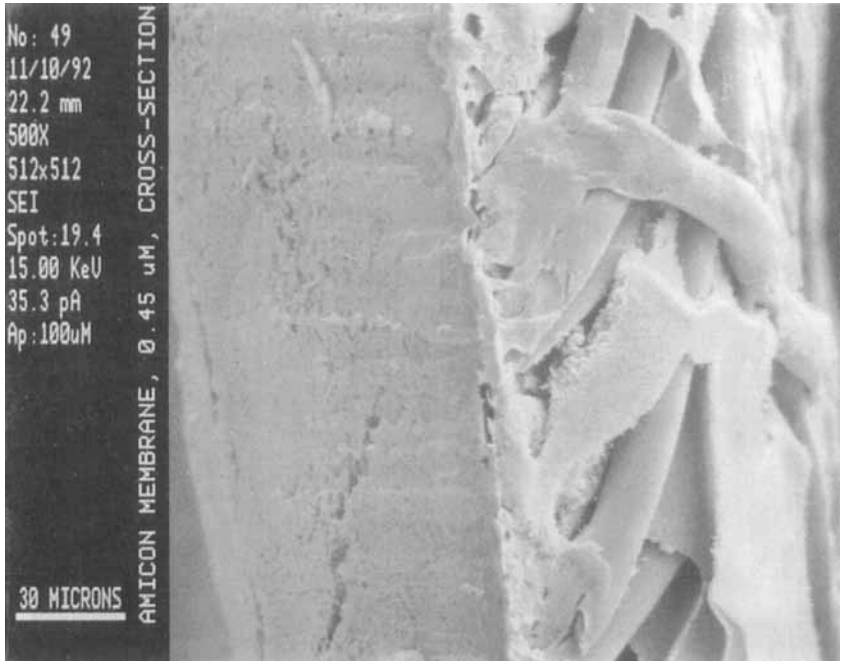

FIG. 11 SEM micrograph of a cross-sectional view of the NC fines deposit layer and fouled membrane.

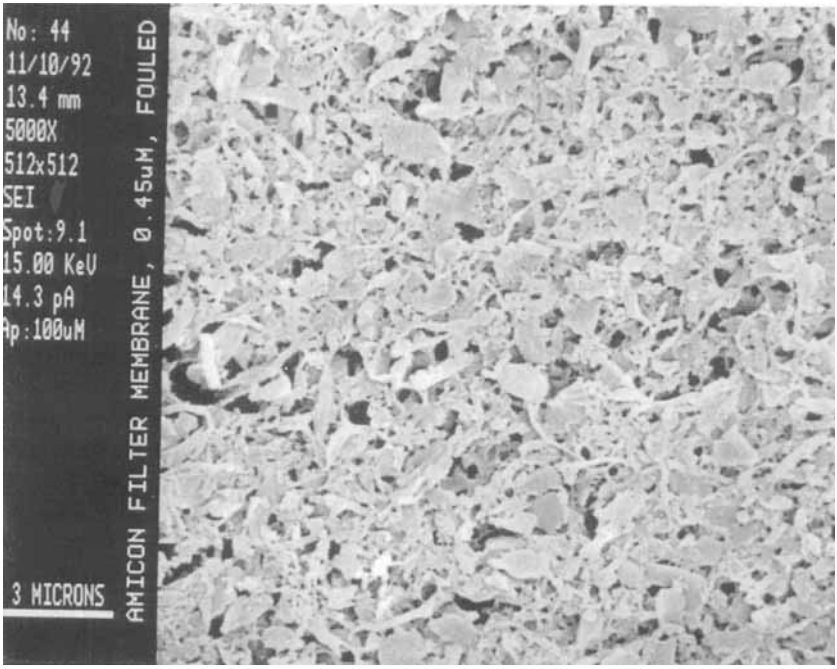

FIG. 12 SEM micrograph of the top view of a fouled M-F membrane.

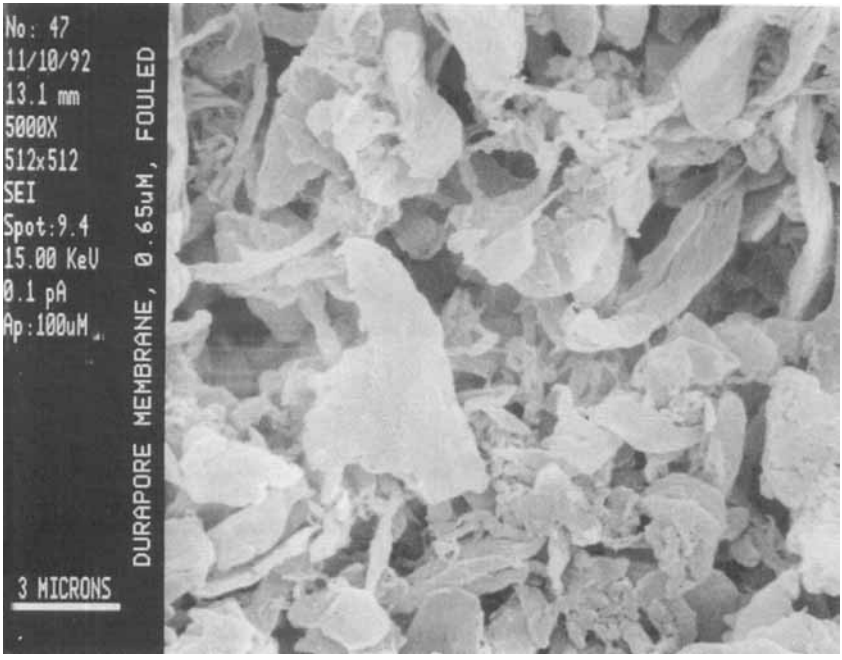

FIG. 13 SEM picture of the deposition of NC fines on the top layer of an M-F membrane.

CONCLUSIONS

The removal of NC fines from NC-manufacturing wastewater was investigated using bench-scale crossflow microfiltration units. It was feasible to separate NC fines from wastewater to almost zero turbidity, indicating that it would not be a problem to meet the effluent limit of 40 mg/L required by NPDES. The particle permeate flux above 100 L/h·m^2 at steady-state or quasi-steady-state could be achieved with the flat-sheet membranes and modules commercially available.

The following conclusions were drawn from the bench-scale flat-sheet crossflow microfiltration experiments:

1. A high crossflow velocity resulted in the reduction of cake layer formation; however, it was not sufficient to deter the membranes from performance deterioration. A crossflow velocity of about 1.07 m/s is recommended for this situation.
2. A higher transmembrane pressure drop could lead to increased membrane fouling resistance for the flat-sheet microfiltration unit separating NC fine suspension. The transmembrane pressure drop should be as low as possible.
3. Microfiltration membrane pores were susceptible to blockage by NC fines due to the wide range of particle size distribution of NC fines.
4. The larger pore size membrane (0.65 μm) performed better than 0.2 and 0.45 μm pore diameter membranes, while all the membranes produced effluents with almost similar turbidities.
5. It was possible to concentrate NC fines to a great extent; however, increased turbidity in the feedwater created a higher membrane fouling rate, suggesting more frequent cleaning.
6. An increase of the permeate flux was observed when pulsating cleaning was applied with an on/off running cycle and interval. A long-term practical permeate flux level could be maintained by incorporating pulsating cleaning technique and chemical cleaning.
7. A model combining the concepts of diffusivity and cake filtration theory was proposed to explain the experimental observations and to understand the physical phenomena governing the permeate flux. Further study is necessary to quantitatively predict the permeate flux by using the equation proposed in this study.

REFERENCES

1. D. O. Helton, *Chemical and Physical Characterization of Nitrocellulose Fines* (AD-AO36-151), U.S. Army Medical Research and Development Command, Washington, D.C., 1976.

2. M. G. Ryan, *Water Quality Criteria for Nitrocellulose* (AD-ORNR-6179), U.S. Army Medical Research and Development Command, Washington, D.C., 1986.
3. Arthur D. Little Inc., *Engineering/Cost Evaluation of Options for Removal/Disposal of NC Fines*, Final Report to USATHMA, 1987.
4. T. Urbanski, *Chemistry and Technology of Explosives*, Vol. 2, Great Britain Reprint, Wheaton, Illinois, 1985.
5. Envirex Inc., *Feasibility Study Regarding Landfilling Nitrocellulose/Lime Sludge and Oxidation of Nitroglycerine Wastewater Stream* (U.S. Army Contract DAAG-53-76-C0082), 1979.
6. J. Barsha, in *Cellulose and Cellulose Derivatives*, 2nd ed. (E. Ott, H. M. Spurlin, and M. W. Grafflin, Eds.), Interscience, New York, 1954.
7. W. A. Lee and R. A. Rutherford, in *Polymer Handbook*, 2nd ed. (J. Brandrup and E. H. Immergut, Eds.), Wiley, New York, 1975.
8. C. W. Nauflett and D. M. French, *Solid Propellant Binders: Quarterly Progress Report (October 1 through December 31, 1973)* (NOL X 73), Naval Ordnance Laboratory, White Oak, Silver Spring, Maryland 20910, 1973.
9. E. J. Siochi and T. C. Ward, *J. Macromol. Sci., 29*, 561 (1989).
10. C.-G. Peng, B. Emmons, X. Shen, and J. K. Park, *Electrophoretic Characteristics and Coagulation/Flocculation of Nitrocellulose-Manufacturing Wastewater, A Report Submitted to Construction Engineering Research Laboratory*, Army Corps of Engineers, 1992.
11. Hercules Inc., *Technical/Financial Performance Report* (Task Order PE-866), February 1991.
12. R. J. Baker, *Desalination, 53*, 89 (1985).
13. G. Schulz and S. Ripperger, *Membr. Sci., 40*, 182 (1989).
14. C. Visvanathan and R. Ben Acm, *J. Membr. Sci., 45*, 6 (1989).
15. G. Belfort and F. W. Altena, *Desalination, 47*, 123 (1983).
16. V. Gekas and B. Hallstrom, *Ibid., 77*, 203 (1990).
17. K. Schneider and W. Klein, *Ibid., 41*, 271 (1992).
18. A. L. Zedney and C. K. Colton, *Chem. Eng. Commun., 47*, 8 (1988).
19. R. Rushton and G. Zhang, *Desalination, 70*, 392 (1988).
20. R. H. Davis and G. A. Birdsell, *Chem. Eng. Commun., 49*, 217 (1987).

Received by editor March 9, 1993